

Seismic and Petrophysical Characterization of Subsurface Reservoirs within Arike Field, Niger Delta, Nigeria

Ayodele Falade¹, John Amigun², Florence Oyediran²

¹ *Department of Geological Sciences, Achievers University Owo, Ondo State, Nigeria*

² *Department of Applied Geophysics, Federal University of Technology Akure, Ondo State, Nigeria*

Received October 7, 2022; Accepted April 3, 2023

Abstract

The study integrated the results from seismic interpretation and petrophysics to describe the properties of identified reservoirs in the subsurface within Arike field, Niger Delta Nigeria. Four wells were correlated and four reservoirs (SAND 1, SAND 2, SAND 3, and SAND 4) were delineated. The petrophysical properties of the reservoirs (lithology, porosity, net sand, net pay, net to gross (NTG), and permeability) were determined. With regard to each reservoir, from SAND 1 to SAND 4, the average values for porosity, permeability, net pay, and NTG were 25.25%, 25.5%, 19.25%, 21.5%; 73.42 md, 51.96 md, 18.25 md, 23.10 md; 12.5 m, 3.53 m, 1.4 m, 3.05 m; and 68.25%, 18.75%, 4.0%, 23.7%. The findings from the study based on reservoir properties reveal that SAND 1 has the best reservoir quality. Ten faults (F1–F10) were mapped using 3D seismic data for structural interpretation of the field, with the majority of them oriented in the NW–SE direction. Seven horizons were picked within the time window of 1.38 s and 1.7 s and their surfaces were generated. At the central part of the map, there is an anticlinal structure that is visible across the surfaces in which the existing wells penetrated. The depth structure map reveals the trapping mechanism to be fault-dependent closure closing against a high and low structure. The study was able to provide subsurface information for future field development by integrating seismic and petrophysics interpretation techniques while also identifying some potential spots on the structural map.

Keywords: *Net pay; Reservoir sand; Seismic; Well logs; Niger Delta.*

1. Introduction

The main natural resource used to produce energy worldwide is petroleum, but the costs and studies involved in its exploration are costly [1]. Exploration leads to the discovery of petroleum, which includes the delineation of reservoirs, followed by the development of the field, and production by primary, secondary, and tertiary oil recovery [2-3]. Uncertainties in oil and gas supplies and unstable prices often lead many companies to focus on increasing their reserves through more precise definition and detailed characterization of reservoirs within oil fields [4-5].

Petrophysical parameters from well log data are fundamental in assessing different possible scenarios within a reservoir [6]. Petrophysical information like lithology, porosity, water saturation, permeability, NTG, volume of shale, etc. are required for proper formation evaluation. These petrophysical information are obtained by integrating several well logs [7-8]. Generally, rock types with low clay content, high porosity, and low irreducible water saturation are more likely to have high reservoir quality, particularly in terms of flow and storage capacity [9].

The seismic survey method is one of the principal methods employed by the petroleum industry for hydrocarbon exploration and recovery to aid production and evaluate the potential of undeveloped areas. Seismic data are useful in the identification of geologic features such as faults and channels leading to the presence of hydrocarbon. One of the importance of seismic data is the identification of subsurface structures that disclose reservoir bodies [10].

Seismic imaging provides detailed lateral and vertical spatial information on reservoir properties that point data like well logs cannot [11].

The results of seismic data analysis are frequently combined with well log analysis to determine how commercially viable a known accumulation is, and it is often planned through reservoir characterization [12-17]. This study is to characterize the subsurface reservoirs by integrating seismic and well log data to show the lateral and vertical information respectively that can be used to guide developmental drilling. The study provides information on the structures and properties of identified reservoirs in the study field which might help in optimising hydrocarbon production.

2. Location and geomorphology of the study area

The field under investigation lies within the onshore Niger Delta in southwestern Nigeria. The Niger Delta is situated in southern Nigeria between latitudes 4°N and 6°N and longitudes 3°E and 9°E [18] as shown in Figure 1.

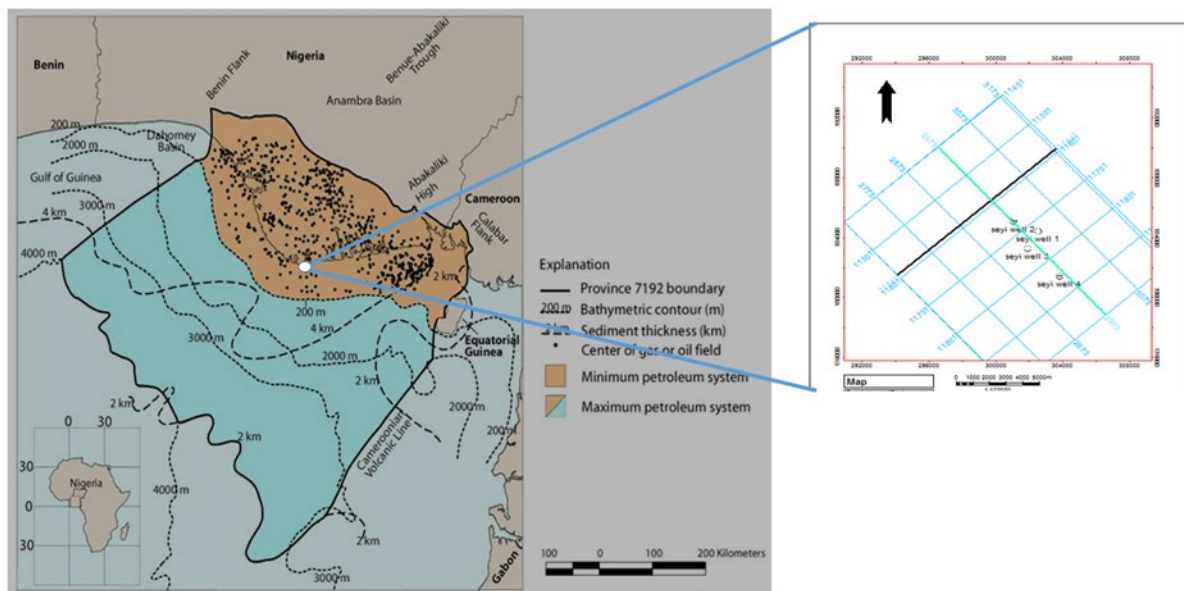


Figure 1. Niger Delta Nigeria showing the study area

2.1. Regional geologic setting of Niger Delta

The Niger Delta is a sedimentary basin that is structurally controlled by lineaments formed when the South Atlantic Ocean opened up [19]. It is located on the Gulf of Guinea in Central Africa's West Coast. According to [20], the NE-SW and NW-SE systems, which define the basin's northern and northeastern edges, respectively, are two structural components that show the existence of the continental Basement. The Benin hinge line refers to the first, while the Calabar hinge line to the second. The Anambra Basin also forms the northern boundary of the basin. Marine sediments started accumulating in the basin in the Albian time after the South Atlantic Ocean opened between the South American and African continents [20]. The Late Paleocene/Eocene accounted for the development of the true delta through building out of sediments across troughs between basement horst blocks on the present delta's northern border. The delta plain has steadily moved southward since then as the oceanic crust assumes a convex shape toward the sea. The structure and stratigraphy of the delta have been influenced by the interaction between subsidence and sediment delivery rates during the course of the delta's geological history [21].

The differential sediment loading on unstable shale and original basement morphology regulates the subsidence, whilst climate fluctuations and eustasy changes influence the pace of sedimentation in the hinterland. Beach, shoreface, channel, and occasionally turbidite sands

from the Akata Formation make up the majority of reservoirs that are currently generating water (Figure 2). Gravity in the delta controls the tectonics of the trap and seal formation. Structural traps have proven to be the most promising exploration target, although stratigraphic traps may hold more significant possibilities in the distal and deeper regions of the delta [22].

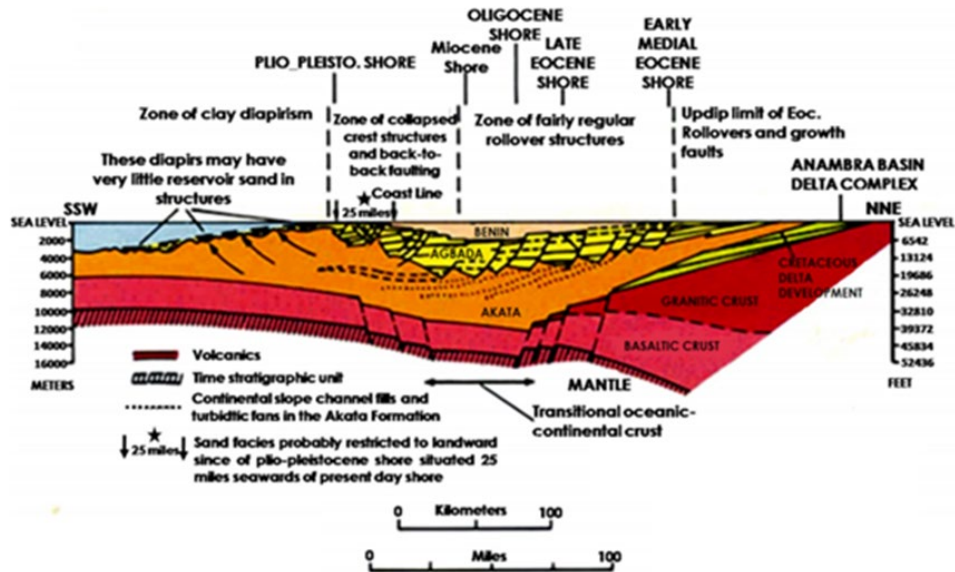


Figure 2. Schematic Dip-Section of Niger Delta with the Three Lithofacies Units, (after [28])

3. Materials and methods of study

3.1. Materials

The database comprised 3D seismic reflection lines covering a field of about 288 km², borehole logs from four wells, velocity check shot survey data, and a base map displaying the wells' location. Petrel™ and Opendtech™ Software with a dedicated workstation were used.

3.2. Methods of interpretation

3.2.1. Base map of the study area

The location, orientation, and distribution of the several data sets are shown on the base map (Figure 3). The map is composed of 3D seismic lines and drilled wells.

3.2.2. Formation evaluation

The well log interpretation involves the extraction of qualitative and quantitative information from geophysical well logs and the computation of petrophysical parameters was accomplished by the transformation of the measured log data into the required formation parameters through the use of standard petrophysical relationship [23]. Interpreted well logs are used in delineating physical rock characteristics like porosity, volume of shale, lithology, identification, and determination of depth and thickness of hydrocarbon-bearing zones [24-25]. The following empirical equations were used in this work to determine reservoir properties:

Volume of shale (V_{sh}) Using the Larionov model [26]

$$V_{sh} = 0.083(2^{3.7 \times I_{GR} - 1.0}) \quad [1]$$

where v_{sh} is the volume of shale; I_{GR} is the gamma ray index and

$$I_{GR} = \frac{GR_{log} - GR_{min}}{GR_{max} - GR_{min}} \quad [2]$$

where GR_{max} is the maximum gamma ray reading (shaly sand); GR_{min} is the minimum gamma ray reading from clean sandstone; GR_{log} is the gamma ray log.

Porosity from density log using matrix and fluid densities according to [23].

$$\phi = \frac{\rho_{ma} - \rho_b}{\rho_{ma} - \rho_{fl}} \quad [3]$$

$$\text{Effective porosity, } \phi_{T-V_{sh}} = \phi_{T-V_{sh}} \quad [4]$$

where ϕ = porosity; ρ_{ma} = matrix density; ρ_b = formation bulk density; ρ_{fl} = fluid density $\phi_{T-V_{sh}}$ = effective porosity (%)

Permeability was calculated mathematically using the equation below.

$$K = \left[\frac{250(\phi)^3}{Sw_{irr}} \right]^2 \quad [5]$$

where ϕ = porosity

$$Sw_{irr} \text{ (irreducible water saturation)} = \sqrt{\frac{F}{2000}} \quad [6]$$

where F (formation factor) = $\frac{a}{\phi^m}$ (a lie between 0.6 and 1 and m is between 1.8 and 2.15)

$$[7]$$

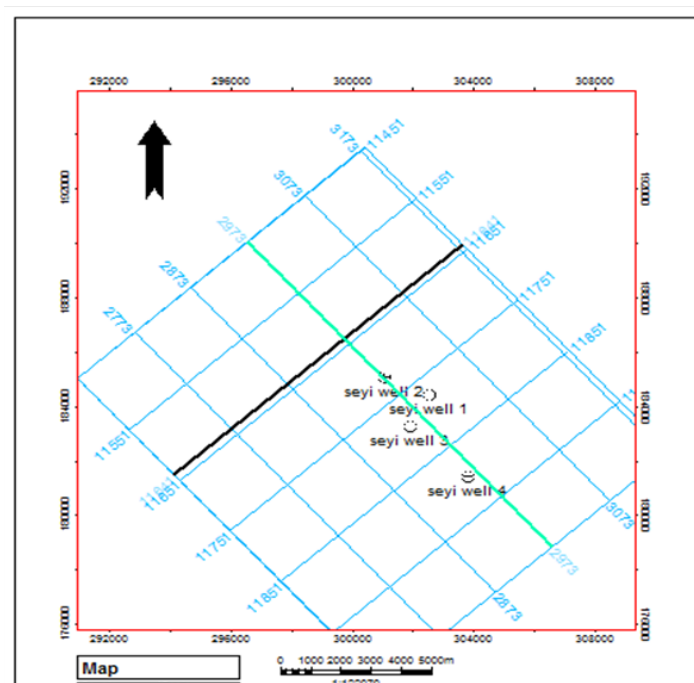


Figure 3. Base map of Field "ARIKE" Showing the positions of the four wells with the inlines and crosslines

3.2.3. Synthetic seismogram

The density and sonic logs were used and combined based on their availability to obtain the reflectivity and impedance, the output of the impedance and reflectivity was convolved with the wavelet gotten from the 3D seismic volume. This was carried out to establish a relationship between well information and seismic data. This is also to effectively correlate the reservoir sands picked on the well log to seismic horizons in order to build a structural-stratigraphic interpretation.

3.2.4. Seismic interpretation

The representation of the physical measurement of the subsurface in the seismic section is displayed in three dimensions of time and space. The Seismic section passed through thorough scrutiny to pick faults, distinguish strong reflections, map horizons, and then prepare seismic maps from the mapped horizons. The strength and continuities of the reflections were used in picking the horizons. Both crosslines and inlines were used for structural interpretation. Fault interpretation was carried out using criteria such as reflection discontinuity at the fault plane, vertical displacement of reflections, and misclosure in tying reflections around loops. Seven

horizons were mapped on both inline and crossline based on amplitude, continuity, coherency, and event strength.

4. Results and discussion

The results of this research work focus on characterizing the reservoirs using well log and seismic data for field development and production planning. Results obtained from this research are presented as tables, graphs, cross-sections, well correlation panel, time maps, and depth maps.

4.1. Identification of lithology/ petrophysical analysis

Figure 4 shows the correlation of the wells in an NW-SE direction. Gamma-ray (GR) log was employed for lithology identification within the wells using a shale baseline of 70 API. Four reservoirs (SAND 1, SAND 2, SAND 3, and SAND 4) were delineated across the wells using gamma ray log and resistivity log. The sand formation mapped was indicated by a deviation to the left from the shale baseline. The lithology consists of the intercalation of shale in sand, when the sand formations correlate with high resistivity reading from the resistivity log, it indicates possible hydrocarbon-bearing sand. Four reservoirs were delineated and analyzed across the four wells, these are labeled in Figure 4. Other reservoir properties were computed from the delineated reservoirs as shown in Table 1.

Sand 1

The thickness of this reservoir across the four wells ranges between 14 m and 24 m, with an average gross thickness of 18 m as seen in table 2. The average volume of shale is 0.035 denoting that this reservoir is almost a clean sandstone across the wells. This reservoir has an average net pay of 12.5 m and an average NTG of 68.25% which shows the presence of hydrocarbon in this reservoir. However, the NTG of this reservoir drops in well 3 and 4 while well 1 has the highest. The average porosity and permeability for this reservoir are 25.25% and 73.42 md respectively. Though this reservoir has the lowest average gross thickness, it has the best quality using the Vsh, net pay, NTG, porosity, and permeability. This reservoir could be targeted for production in all the wells drilled in the study area based on their quality per well.

Sand 2

This reservoir's thickness varies between 14 and 27.5 m across the four wells, with an average gross thickness of 20.63 m (Table 2). With an average volume of shale of 0.0625, the shale content indicates that this reservoir is fairly similar in cleanliness to sand 1. The best reservoir of sand 2 was discovered in well 1 out of the four wells, with an average net pay of 3.53 m and an average NTG of 18.25%. The reservoir in well 4 has 0.00 NTG, which means there are no hydrocarbons present in that specific reservoir. This reservoir has an average porosity and permeability of 25.5% and 51.96 md, respectively. Using the Vsh, net pay, NTG, porosity, and permeability, this reservoir has a relatively good quality. Based on the quality of each well, only wells 1 and 3 in the study area should be targeted for the production in sand 2.

Sand 3

As shown in table 2, the thickness of this reservoir varies between 31 and 37.5 m across the four wells, with an average gross thickness of 33.63 m. With an average volume of shale of 0.115, Sand 3 is the dirtiest reservoir in all the wells. The average net pay and average NTG for this reservoir are 1.4 m and 4.0%, respectively, indicating that the majority of the reservoir is filled with water, with the exception of well 3, which has an NTG value of 16%. For this reservoir, the average permeability and porosity are 19.25% and 18.25 md, respectively. The quality of this reservoir, despite having the highest average gross thickness, is the lowest when compared to other reservoir characteristics. Based on their quality per well, only well 3 in the study area could be targeted for production from this reservoir.

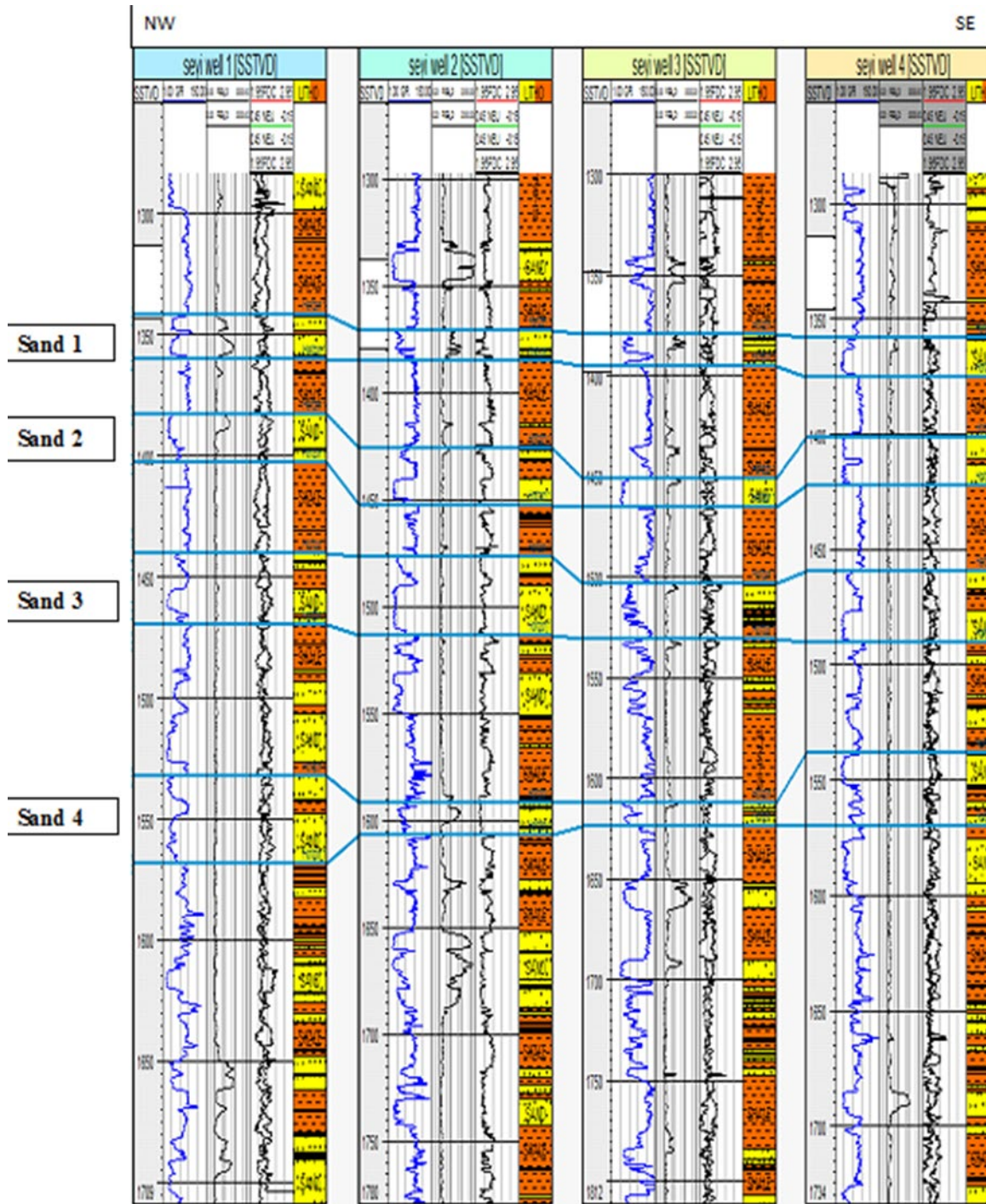


Figure 4. Well correlation panel of "ARIKE" Field

Sand 4

The thickness of this reservoir varies between 12 and 37 m across the four wells, with an average gross thickness of 23.5 m (table 2). This reservoir is only slightly cleaner than sand 3, as indicated by the average volume of shale being 0.10. This reservoir has an average net pay of 3.05 m and an average NTG of 23.75%, with well 2 having the best quality of this among SAND 4 in all of the four wells. However, this reservoir in wells 1 and 4 has 0.00 NTG, indicating that there is no hydrocarbon present. For this reservoir, the average porosity and permeability are 21.5% and 23.10 md, respectively. Using the gross thickness, V_{sh} , NTG,

porosity, and permeability, this reservoir generally has a fair quality. Based on their quality per well, the only Sand 4 in the study area that could be selected for production in well 2.

Table 1. Summary of petrophysical parameters computed for the wells

Well No	Reservoir sands	Gross thickness (m)	Net pay (m)	NTG (%)	V _{shale} (%)	Total ϕ (%)	PhiE (%)	K (md)
Well 1	Sand 1	24	22.3	93	2	20	18	88.9
	Sand 2	20	8.9	45	3	26	21	54.66
	Sand 3	31	0	0	5	22	19	30.45
	Sand 4	37	0	0	3	23	20	45.97
	Average	28	7.8	34.5	3.25	22.75	19.5	55.00
Well 2	Sand 1	14	14	100	2	27	23	110.25
	Sand 2	27.5	2	7	14	18	15	14.03
	Sand 3	37.5	0	0	11	19	16	14.96
	Sand 4	13	10.2	78	8	25	21	26.23
	Average	23	6.55	46.25	8.75	22.25	18.75	41.37
Well 3	Sand 1	17	7.7	45	7	27	23	38.27
	Sand 2	14	3.2	23	1	29	28	119.57
	Sand 3	35	5.6	16	17	18	11	12.62
	Sand 4	12	2	17	10	22	17	11.69
	Average	19.5	4.625	25.25	8.75	24	19.75	45.54
Well 4	Sand 1	17	6	35	3	27	24	56.27
	Sand 2	21	0	0	7	29	22	19.57
	Sand 3	31	0	0	13	18	15	14.96
	Sand 4	32	0	0	19	16	12	8.49
	Average	25.25	1.5	8.75	10.5	22.5	18.25	24.82

Table 2. Summary of the Evaluated Sands across the Wells in 'Arike" Field

Reservoir sands	Avg gross thickness (m)	Avg net pay (m)	Avg NTG (%)	Avg V _{sh} (%)	Avg total ϕ (%)	Avg PhiE (%)	Avg K (md)
SAND 1	18	12.5	68.25	3.5	22.25	22	73.42
SAND 2	20.63	3.53	18.75	6.25	25.5	21.5	51.96
SAND 3	33.63	1.4	4.0	11.5	19.25	15.25	18.25
SAND 4	23.5	3.05	23.75	10	21.5	17.5	23.10

4.2. Synthetic seismogram generation

The synthetic seismogram shows a better connection between the seismic section and well log. The combination of density and sonic logs gives acoustic impedance and reflectivity. Each horizontal signal line on the seismic section represents the amplitude strength, the output of the log signature which gives events on the seismic section that correspond to the geologic formation on the well log. The output is a synthetic seismic trace for Arike well 4 as shown in Figure 5. Horizons 1-7 were matched with the seismic trace extracted in the volume along the well path so as to ensure correct interpretation of the process started from the known to the unknown. Both composite seismic and synthetic traces were cross-correlated to get an indication of the alignment and matching quality as an output value. There was little or no need for alignment of the seismic and synthetic traces since there was little or no difference in the travel time.

4.3. Fault picking and horizon mapping

The structural interpretation of the field was based on analyses of mapped faults and horizons from the seismic sections. Figure 6 shows the typical section showing faults and horizons mapped in the study area. The seismic volume inline number is between 11451 and 12051 while the crossline number is between 2673 and 3180. Ten faults marked F1 to F10 were mapped in the field (Figure 6). The major fault dips towards NW - SE direction with the

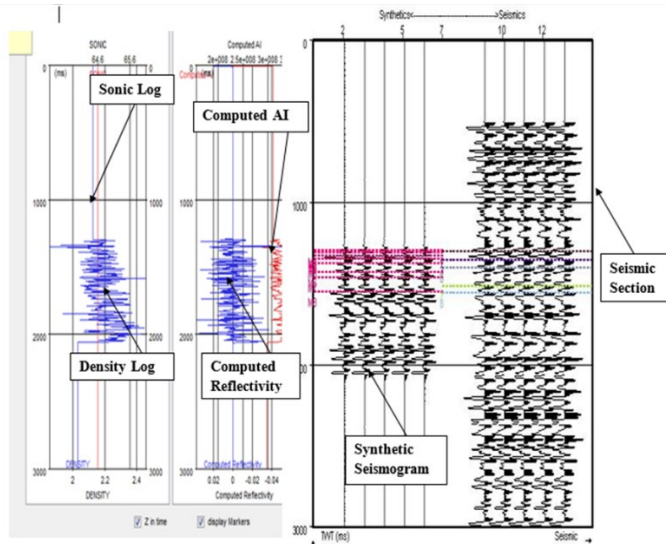


Figure 5. Synthetic Seismogram for Well 4

angle increasing with depth and minor fault in the northeast direction. The section is characterized by structural building faults and the reflection events (H1 – H7) are displayed in the section. F1 and F9 are antithetic faults dipping in an opposite direction to the major faults whereas the other faults mapped show curved and concave-upward fault planes in the down-dip direction, their slope progressively decreases until they became horizontal or flat with depth, suggesting they are growth faults. The horizon mapped falls within the window of 1.34 to 1.65 seconds. The seismic sections possess a bad character after 1.65 s suggesting maybe a shale diapir is responsible.

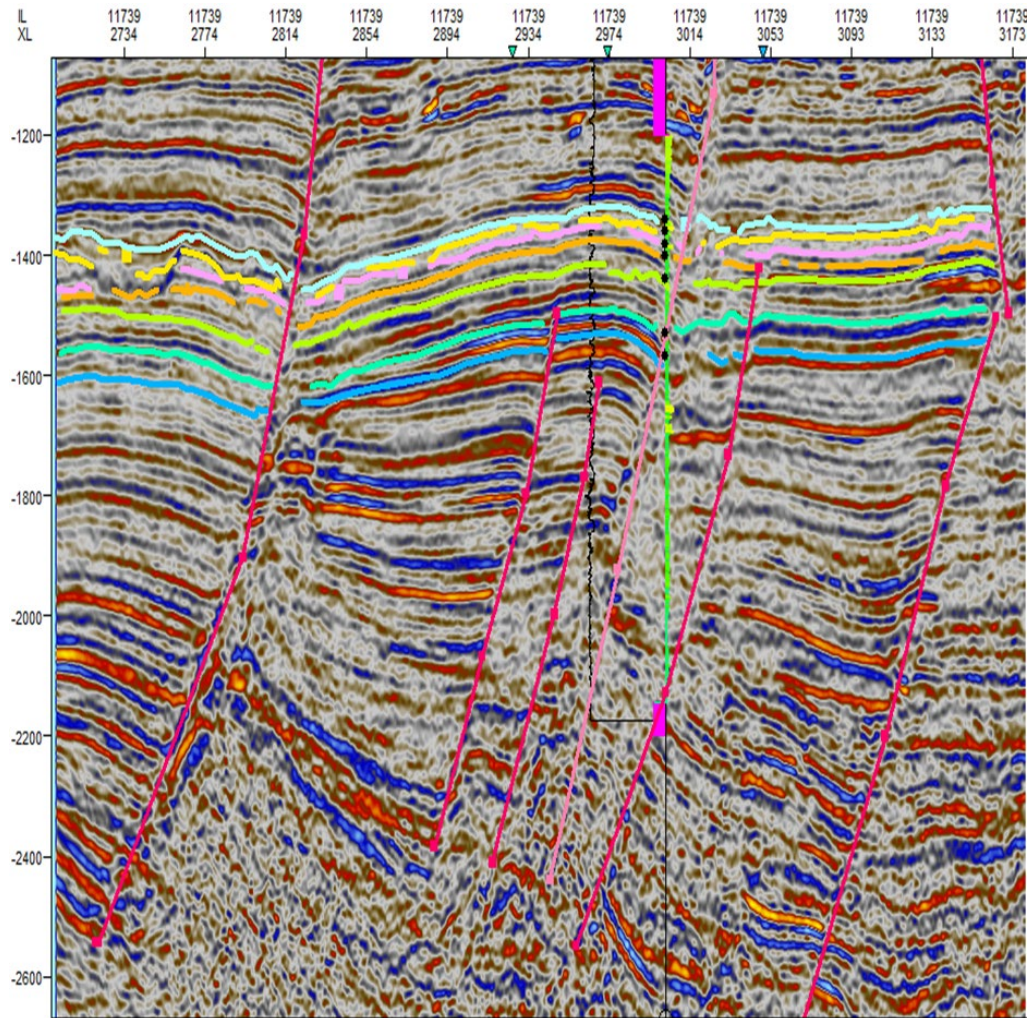


Figure 6. Mapped Faults and Horizons on Inline 11739 (Petrel 2010 Version)

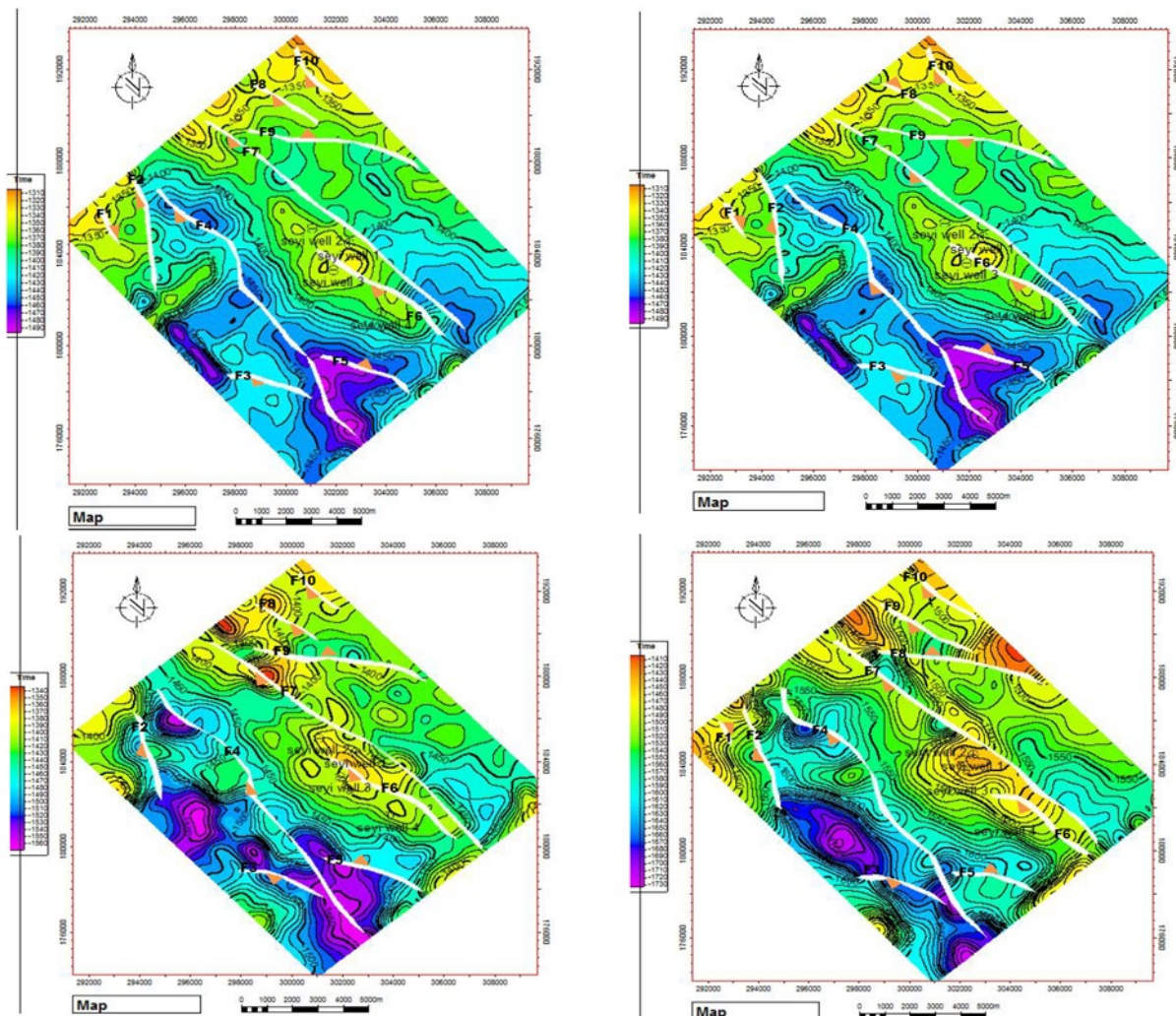
4.4. Structural maps

The structural maps generated for the field as shown in Figures 7a - 7g shows the various Time Structural maps of Horizons 1 to 7, while Figure 8 shows the Time-Depth graph used in converting the seismic two-way time to the depth structural maps in Figures 9a - 9g and the summary of the depth surfaces is shown in Table 3.

4.4.1. Time structure map of horizons

Figures 7a indicate the time structure map of horizon 1 having a time range of 1.3 s to 1.49 s and a contour interval of 50 m. The time slice shows colour variations that are used to describe the map (orange, yellow, green, blue, and purple). The mapped faults (F1 - F10) are seen on the time slice. F1, F5, and F9 dip in the northeast direction while the remaining fault dips towards the direction north-south. At the central part of the map is an anticlinal structure closing against F6, and a bigger closure closing against F7 which the existing well penetrated. Some other closures are also seen but are classified within structurally low areas.

Horizon 2 displays a time range of 1.31 to 1.5 seconds the contour interval is 50 m (Figure 7b). The time variation can be observed using the colour bar. The map still shows the identified faults. The centre of the map shows a fault-dependent closure that the existing well is targeting; this could be a potential hydrocarbon accumulation. Additionally, the northeastern region of the map shows that the area is structurally high, indicating that the hydrocarbons in the area are structurally restricted.



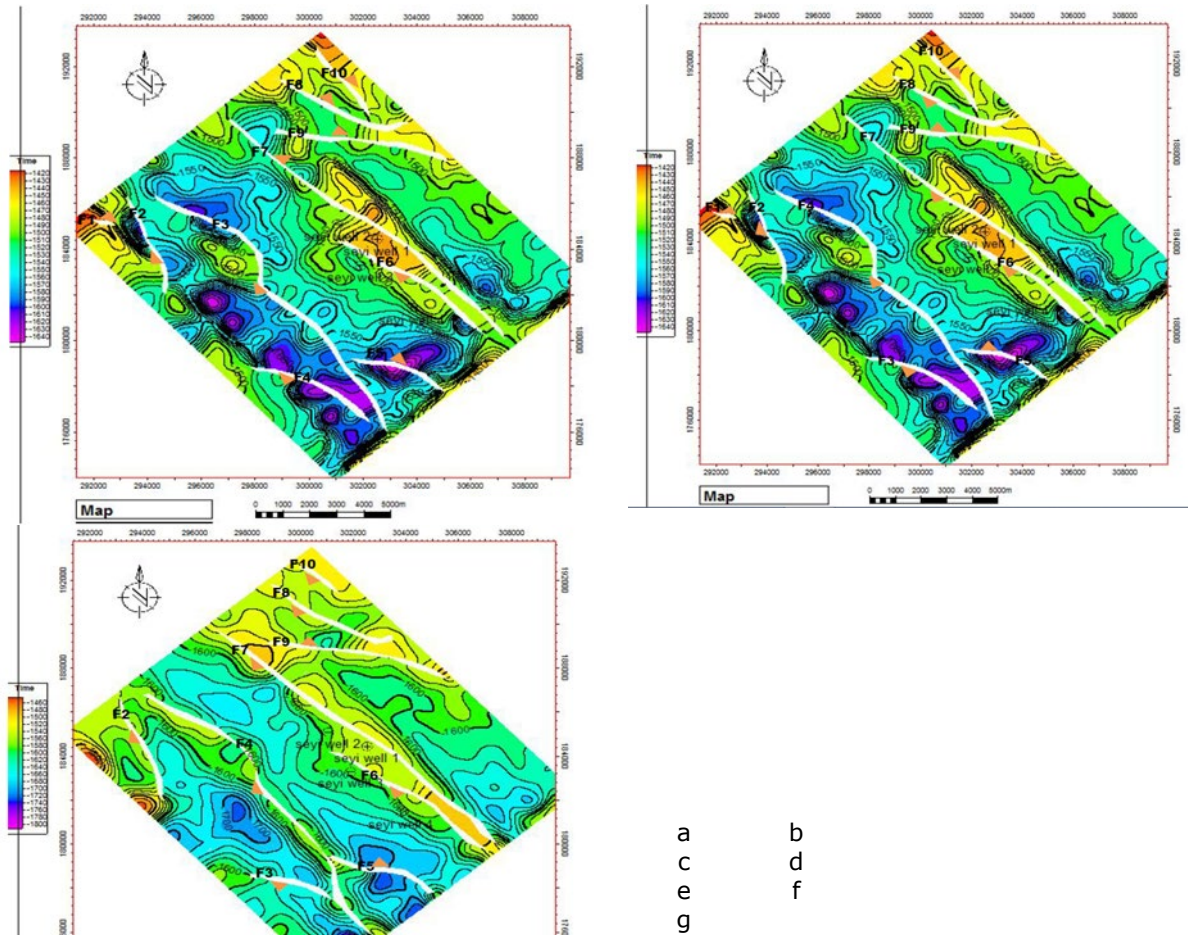


Figure 7. Time Map Showing Mapped Faults (F1 – F10) and Direction of Dip (▲) for (a) Horizon 1 (b) Horizon 2 (c) Horizon 3 (d) Horizon 4 (e) Horizon 5 (f) Horizon 6 (g) Horizon 7

Figure 7c in Horizon 3 depicts a range in the time at which the map was formed semicolon from 1.34 to 1.56 seconds. The north-eastern part shows the area is structurally high and the central part of the study still reveals a fault-dependent which the four existing well penetrated. Another closure is seen, although it occurs in the structurally weak region to the south.

In Horizon 4, the map generation duration varies, ranging from 1.41 to 1.6 seconds (Figure 7d) with 50 m separate each contour. The middle region of the map still exhibits an anticlinal pattern. On the map, there is still another closure closing up with F4, further demonstrating that the structures are in control of the local hydrocarbon accumulations.

The time structure map for horizon 5 is shown in Figure 7e, with a time range between 1.42 s and 1.64 s. The faults that may be observed on the map are still obvious. The four drilled wells are still located within the primary anticlinal structure that was the target. Still evident are certain closures that might represent a structure that could hold hydrocarbon.

Figures 7f show the time structure map for horizon 6 with time range of 1.44 and 1.76 s and a 100 m contour interval. Two of the four wells lack the targeted anticlinal structure for the accumulation of hydrocarbons because the required anticlinal structure is less obvious on the map. Additionally, the maps exhibit fault-assisted and fault-dependent closures.

The time structure map of horizon 7 with a time range of 1.45 s and 1.8 s is shown in Figure 7g. 100 m separate each contour. The time structural maps of the horizons show the same pattern of severe structural deformation throughout time.

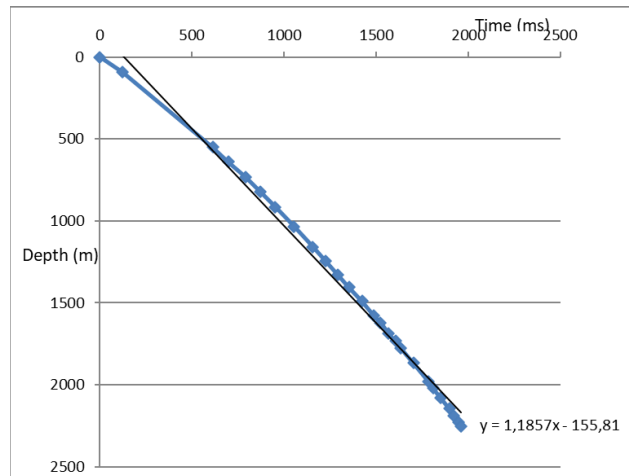
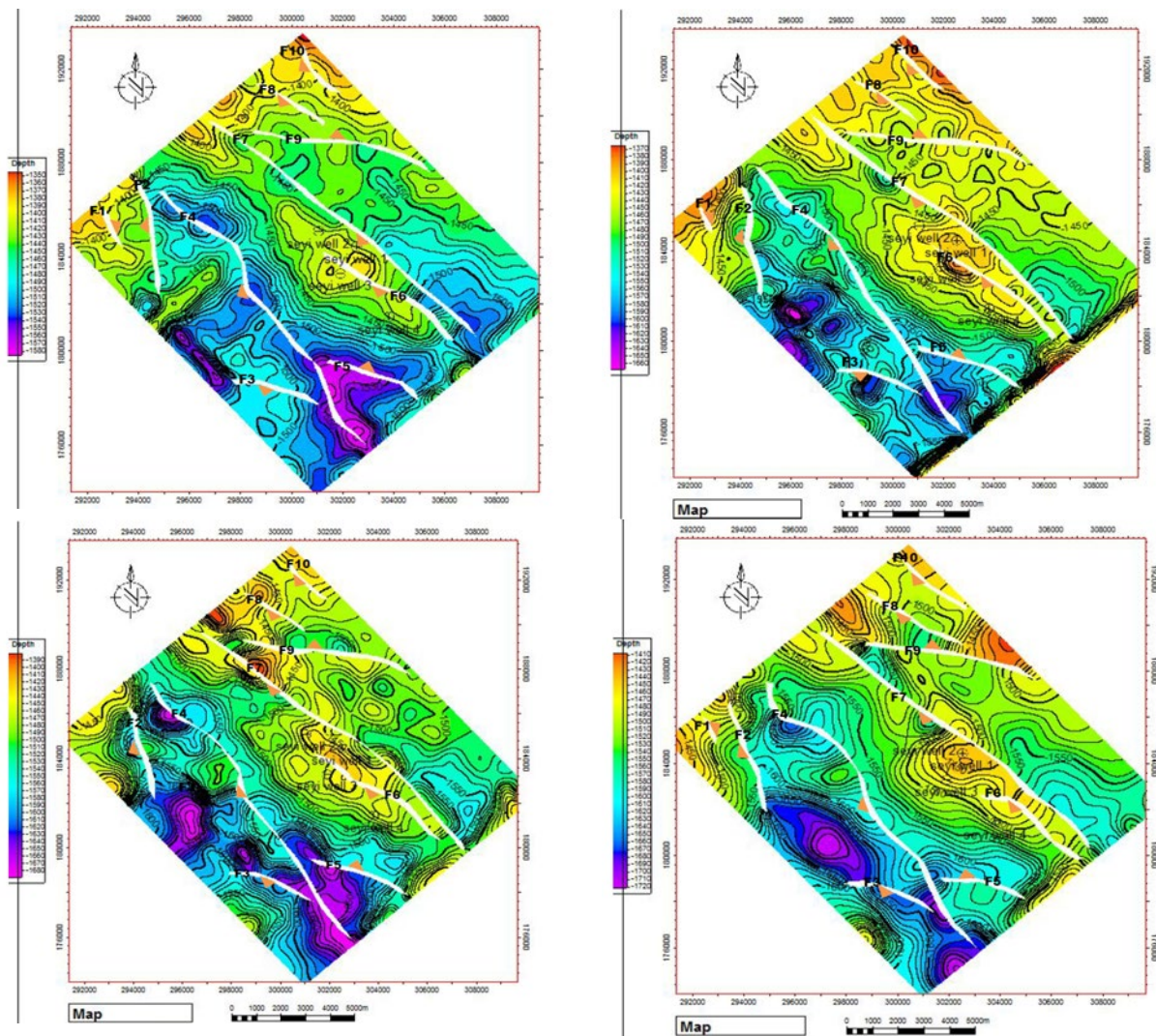


Figure 8. Time-Depth conversion graph



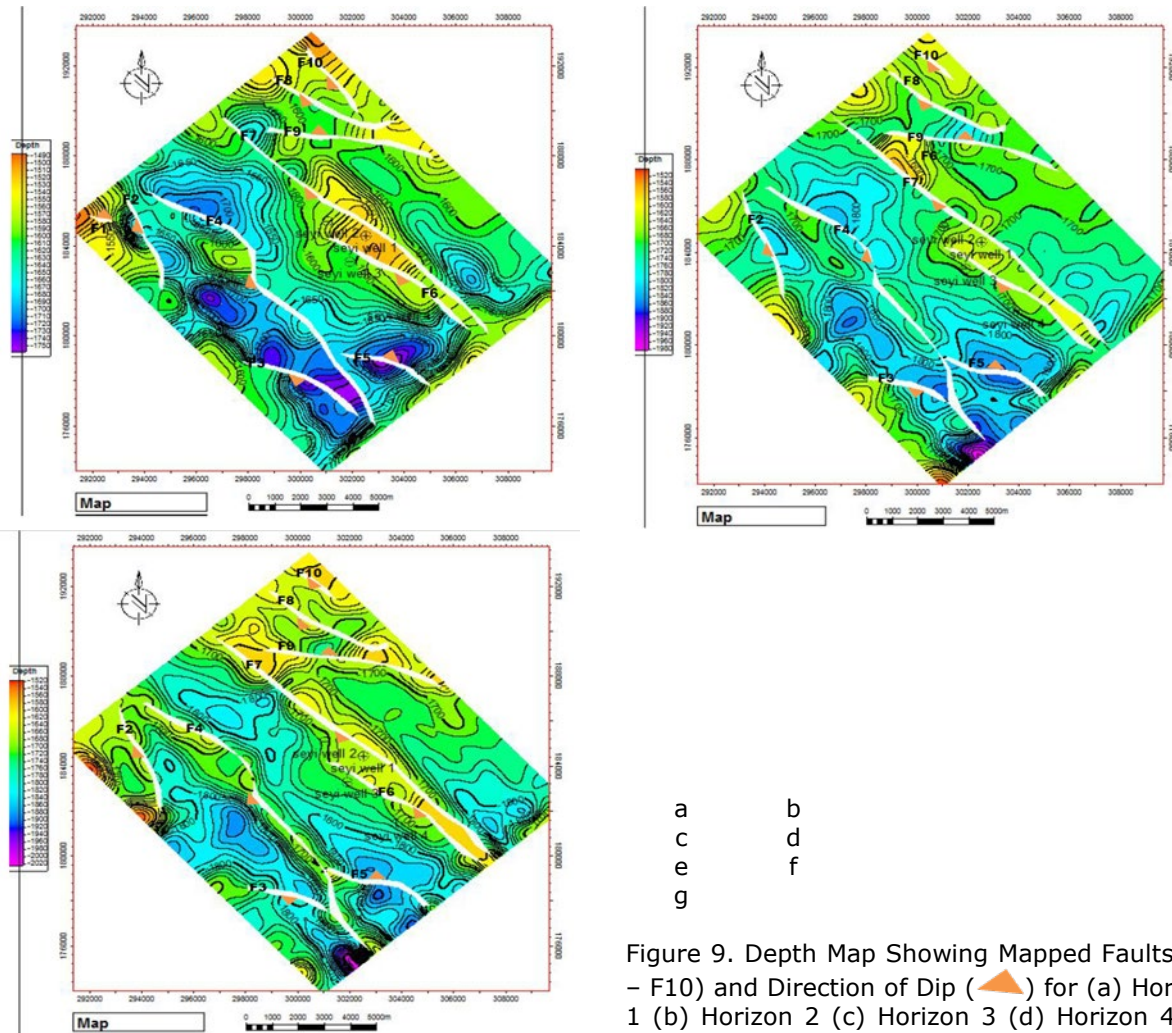


Figure 9. Depth Map Showing Mapped Faults (F1 – F10) and Direction of Dip (▲) for (a) Horizon 1 (b) Horizon 2 (c) Horizon 3 (d) Horizon 4 (e) Horizon 5 (f) Horizon 6 (g) Horizon 7

Table 3. Summarized detail of the depth surface horizons

Horizon	Depth range (m)	Contour interval (m)
1	1350 – 1580	50
2	1370 – 1660	50
3	1390 – 1680	50
4	1410 – 1720	50
5	1490 – 1750	50
6	1520 – 1980	50
7	1520 – 2020	100

5. Conclusion

Four wells were used to determine the petrophysical parameters in the Arike field, where a total of 600 in-lines and 507 cross-lines were analysed for this study project. A detailed fault mapping reveals that the area is highly faulted with majority of the faults in the NW – SE direction. The formation evaluation result reveals that sand 1 has the best reservoir quality based on its properties and could be targeted in all four wells during production. The results showed that a reservoir's gross thickness is irrelevant if it has a low value for significant characteristics like the net to gross calculated using net pay which is a reflection of its hydro-carbon content. In order to assess the reservoir quality, this study chose a petrophysical study of net pay as one of the key reservoir properties to be established. Additionally, it is discovered

that not all identified reservoirs might be selected for production, demonstrating the heterogeneity of the subsurface. The surfaces generated from seismic section an anticlinal structure at the centre part that the existing wells penetrated. The drilling of these wells indicates that this structure was a target. Depth variation in the surface maps also shows that the sediments have suffered a higher degree of deformation. The trapping mechanism is revealed by the depth structure map to be fault-dependent closure closing against high and low structures. In general, the information extracted reveals a detailed understanding of the subsurface, providing essential information required for subsurface evaluation, and hydrocarbon recovery which could also be applied in deciding potential areas to be drilled.

Statements & declarations

Funding

No funding was made available for this research. It was funded by the authors.

Competing interests

The authors declared that they have no competing interests.

Authors contributions

Ayodele Falade: *Conceptualization, Methodology, Software, Visualization, Investigation, Writing-Reviewing, and editing.* **John Amigun:** *Visualization, Investigation, Software, Validation, Editing, Supervision.* **Florence Oyediran:** *Investigation, Software, Data curation, Validation, Writing.*

References

- [1] Tietenberg T, Lewis L. Environmental and natural resource economics. Routledge, 2018.
- [2] Satter A, Iqbal G. Reservoir engineering: the fundamentals, simulation, and management of conventional and unconventional recoveries. Gulf Professional Publishing, 2015.
- [3] Kafisanwo O, Falade A, Bakare O, Oresanya A. Reservoir characterization and prospect identification in Onka field, offshore, Niger Delta. Environmental and Earth Sciences Research Journal, 2018; 5(4): 79-86.
- [4] Kafisanwo O, Abe J, Falade A. Generating pseudo-synthetic seismogram with resistivity logs considering the effect of gas: Application to Bizzy field, onshore, Niger-delta, Nigeria. Environmental and Earth Sciences Research Journal, 2019; 6(4): 149-161.
- [5] Abuhagaza A, El Sawy M, Nabawy B. Integrated petrophysical and petrographical studies for characterization of reservoirs: a case study of Muglad Basin, North Sudan. Environmental Earth Sciences, 2021; 80(5): 1-18.
- [6] Bosch M, Mukerji T, Gonzalez E. Seismic inversion for reservoir properties combining statistical rock physics and geostatistics: a review. Geophysics, 2010; 75(5): A165-A176.
- [7] Oyekan A, Issa T. Reservoir Modelling Using Seismic Attributes and Well Log Analysis of "OAK Field", Niger Delta, Nigeria. International Journal of Geography, Geology & Agricultural Research, 2017; 1(1): 11-24.
- [8] Falade A, Ijato S, Edema A, Oni T. Evaluation of Reservoir Sand using Petrophysical Analysis in 'Jat' Field, Niger Delta Basin Nigeria. Achievers Journal of Scientific Research, 2021; 3(2): 1-18.
- [9] Al-Baldawi B. Petrophysical evaluation study of Khasib formation in amara oil field, South Eastern Iraq. Arabian Journal of Geosciences, 2015; 8(4): 2051-2059.
- [10] Chapin M, Swinburn P, Van der Weiden R, Skaloud D, Adesanya S, Stevens D, Varley C, Wilkie J, Brentjens E, Blaauw M. Integrated seismic and subsurface characterization of Bonga Field, offshore Nigeria. The Leading Edge, 2002; 21(11): 1125-1131.
- [11] Li Z, Qu Y. Research progress on seismic imaging technology. Petroleum Science, 2022; 19(1): 128-146.
- [12] Moore I. Alba Field—how seismic technologies have influenced reservoir characterization and field development. Geological Society, London, Special Publications, 2015; 403(1): 355-379.
- [13] Opara A. Prospectivity evaluation of "Usso Field", Onshore Niger Delta basin using 3-D seismic and Well log data. Petroleum and Coal, 2010; 52(4): 307-315.
- [14] Islam M, Yunsi M, Qadri S, Shalaby M, Haque A. Three-dimensional structural and petrophysical modeling for reservoir characterization of the Mangahewa Formation, Pohokura Gas-Condensate Field, Taranaki Basin, New Zealand. Natural Resources Research, 2021; 30: 371-394.

- [15] Obimma K, Obiora D, Oha A, Ibuot J, Yakubu J. Seismic and Petrophysical Characterization of Reservoirs in Kjoe Field, On-Shore Niger Delta, Nigeria. *Petroleum and coal*, 2021; 63(1): 50-62.
- [16] Okoli A, Agbasi O, Lashin A, Sen S. Static reservoir modeling of the Eocene clastic reservoirs in the Qfield, Niger Delta, Nigeria. *Natural Resources Research*, 2021; 30: 1411-1425.
- [17] Falade A, Amigun J, Makeen Y, Kafisanwo O. Characterization and geostatistical modeling of reservoirs in 'Falad' field, Niger Delta, Nigeria. *Journal of Petroleum Exploration and Production Technology*, 2022; 12(5): 1353-1369.
- [18] Nwachukwu J, Chukwura P. Organic matter of Agbada Formation, Niger Delta, Nigeria. *AAPG bulletin*, 1986; 70(1): 48-55.
- [19] Knox G, Omatsola E. Development of the Cenozoic Niger Delta in terms of the "Escalator Regression" Model and Impact on Hydrocarbon Distribution. *Coastal Lowland: Geology and Geotechnology*, 1989; 181-202.
- [20] Murat R. Stratigraphy and paleogeography of the Cretaceous and Lower Tertiary in Southern Nigeria. *African geology*, 1972; 1(1): 251-266.
- [21] Edwards J, Santogrossi P. Divergent/Passive Margin Basins American Association of Petroleum Geologists Memoir 48, 1990; 201-238
- [22] Tuttle M, Charpentier R, Brownfield M. The Niger Delta Petroleum System: Niger Delta Province, Nigeria, Cameroon, and Equatorial Guinea, Africa. US Department of the Interior, US Geological Survey, 1999; 99-50.
- [23] Asquith G, Gibson C. Basic well log analysis for geologists. Tulsa: American Association of Petroleum Geologists, 1982; 3.
- [24] Gogoi T, Chatterjee R. Estimation of petrophysical parameters using seismic inversion and neural network modeling in Upper Assam basin, India. *Geoscience Frontiers*, 2019; 10(3): 1113-1124.
- [25] Pandey A, Chatterjee R, Choudhury B. Application of neural network modelling for classifying hydrocarbon bearing zone, water bearing zone and shale with estimation of petrophysical parameters in Cauvery basin, India. *Journal of Earth System Science*, 2020; 129(1): 1-17.
- [26] Larionov V. Radiometry of boreholes (in Russian). Nedra, Moscow, 1969; 127

To whom correspondence should be addressed: Ayodele Falade, Department of Geological Sciences, Achievers University Owo, Ondo State, Nigeria, E-mail: ayouseh2003@gmail.com